

# Unsupervised Imitation Learning

Sebastian Curi      Kfir Y. Levy      Andreas Krause

Department of Computer Science, ETH Zurich

## Abstract

We introduce a novel method to learn a policy from unsupervised demonstrations of a process. Given a model of the system and a set of sequences of outputs, we find a policy that has a comparable performance to the original policy, without requiring access to the inputs of these demonstrations. We do so by first estimating the inputs of the system from observed unsupervised demonstrations. Then, we learn a policy by applying vanilla supervised learning algorithms to the (estimated)input-output pairs. For the input estimation, we present a new adaptive linear estimator (AdaL-IE) that explicitly trades-off variance and bias in the estimation. As we show empirically, AdaL-IE produces estimates with lower error compared to the state-of-the-art input estimation method, (UMV-IE) [Gillijns and De Moor, 2007]. Using AdaL-IE in conjunction with imitation learning enables us to successfully learn control policies that consistently outperform those using UMV-IE.

## 1 Introduction

In imitation learning, the goal is to learn a "useful" policy from demonstrations of a teacher. This field is divided into inverse reinforcement learning and behaviour cloning. Inverse reinforcement learning algorithms fit a reward function that explains the teacher's behaviour under the assumption that it is (near) optimal and it generalizes to unseen state-action pairs [Abbeel and Ng, 2004]. After fitting the reward function, the whole markov decision process (MDP) must be solved to find the optimal policy [Kober et al., 2013]. The main drawbacks of this approach are that it assumes near optimality of the demonstrations, which might not be true, and the need to solve an MDP once the reward is learned, which is computational expensive. Moreover, even under the optimality assumption, the problem of learning the reward function is ill-posed since there may be several very different such functions that explain the teacher's behaviour.

Behavioural cloning fits a policy from observed input-output pairs and does not require the optimality assumption [Ross et al., 2011]. This approach does not adapt to changing environments and, when the learning agent encounters an unvisited states, it needs to query a teacher, or it may perform arbitrarily badly.

While both of these approaches have been successfully applied to real-world systems, there are still major limitations in applying them to complex processes. Consider, for example, the

task of policy learning for self-driving cars. Performing a controlled experiment with an expert driver that *teaches* the learning agent which actions it should do is very time-consuming and expensive [Bojarski et al., 2016]. On the other hand, there is a huge amount of recording of surveillance cameras with car trajectories. Clearly, this data cannot be used in any of the methods presented above because it does not contain the inputs the driver used, e.g., steering angle and accelerating or breaking forces.

In this paper, we take a different approach. Instead of querying a teacher, we directly estimate the actions of a teacher from observed demonstrations (outputs). Then, we use these input-output pairs together with standard imitation learning in order to learn a good policy. As we show in this paper, existing input estimation methods suffer from high variance and are not appropriate to be used with imitation learning approaches. Thus, we develop a novel input estimation method, AdaL-IE, which explicitly trades off bias for variance and achieves a lower estimation error compared to UMV-IE, the state-of-the-art approach. Using AdaL-IE estimates as targets for imitation learning, we successfully learn policies without any expert supervision.

## Related Work

**Input Estimation:** In input estimation problems we receive the outputs of dynamical system and the objective is to recover the inputs signals that generated these outputs. Methods which assume the knowledge of the dynamics usually construct *unbiased* estimates for the input signals. This is done in the spirit of Kalman Filtering, i.e., given the dynamics and further assuming Gaussian measurement and process noise, one can solve the Maximum Likelihood estimator for the inputs. One of this first method in this spirit was derived in Corless and Tu [1998]. However, they only provide asymptotic guarantees on the accuracy of the estimator. On the other hand, the method presented later in Gillijns and De Moor [2007] presents a minimum variance *unbiased* estimate of the input. Their method, UMV-IE (unbiased minimum variance input estimator), is the method of choice in current applications [Anagnostou and Pal, 2018, Girardin et al., 2010, Park and Altintas, 2004]. Similar ideas were later investigated in Bolliger et al. [2013], and in Maes et al. [2018]. In contrast to these works we do not assume Gaussian measurement and process noise, and do not limit ourselves to unbiased input estimates. As we show in the experiments, this yields a smaller estimation error which in turn enables to learn better policies when we combine these estimates with imitation learning procedures.

**Imitation Learning:** Imitation learning relates to methods in which a policy is learned by querying a teacher (for an extensive survey of the literature see e.g., [Schaal, 1999, Billard et al., 2008, Argall et al., 2009, Hussein et al., 2017]).

Learning directly from observations (without direct access to actions) is a recent line of research introduced in Liu et al. [2017]. In this work, the authors observe demonstrations produced in different contexts, and translating between contexts they recover a reward function for feature tracking. They use this reward function in an MDP setting to find the optimal policy in an inversed reinforcement learning fashion. Finally, there has been recent

efforts to use behavioral cloning algorithms for imitation learning when actions are not known. In [Edwards et al. \[2018\]](#), the authors present model free approach for discrete states and actions, and consists of two steps: a first step that finds the action that best predicts the observed state transition, and a second step that, by interacting with the environment, corrects the model of the system used to infer this action. In [Torabi et al. \[2018\]](#), the authors first learn a model that maps state transitions to actions by interacting with the environment. Then, from demonstrations where only states are observed, they infer actions from the state transitions using the learned model and fit a policy by mapping the states to this inferred actions. These methods are both model free and work either for discrete actions, or assuming a (Gaussian) distribution over the action space in the continuous case. In our paper, we take a model-based approach and is applied in a continuous state and action space without assuming any prior on the action distribution. The model based approach is critical when the observation comes from a video or an external source, where there are no possibilities to interact with the environment to infer the actions.

**Our Contribution:** We introduce a novel method for imitation learning of continuous continuous system that does not require access to the input demonstration of an expert. For this, we present a novel adaptive estimator that is linear on the measurements. Instead of using a Kalman filter style analysis, we relax the estimation error, in which bias and variance terms appear explicitly. We show that this relaxation translates to a convex optimization problem that may be solved efficiently. We use our estimates as the imitation learning targets to successfully learn a policy through behaviour cloning.

## 2 Background, Assumptions, and Problem Statement

In this section, we introduce linear time invariant dynamical systems. We state our goal together with the assumptions used throughout this work. In [Section 4.3](#) we extend our approach to a wider class of non-linear time variant dynamical systems.

**Notation:** A vector  $v_t \in \mathbb{R}^n$  denotes a vector  $v$  at time step  $t$ , and  $v_{t_1:t_2}$  a sequence of vectors  $\{v_{t_1}, v_{t_1+1}, \dots, v_{t_2-1}, v_{t_2}\}$ . We indicate  $i$ -th entry of a vector at time step  $t$  as  $v_t[i] \in \mathbb{R}$ . For a matrix  $A \in \mathbb{R}^{n \times m}$ , the Moore-Penrose pseudo inverse is  $A^\dagger = (A^\top A)^{-1} A^\top$ . We use  $\|\cdot\|$  to denote the 2-norm of a vector, or the induced 2-norm (a.k.a. spectral norm) of a matrix.

**Linear Dynamical Systems** [[Franklin et al., 1998](#)]. A linear time-invariant dynamical system can be parametrized with matrices  $(A, B, C)$ . The state  $x_t \in \mathbb{R}^{n_x}$ , input  $u_t \in \mathbb{R}^{n_u}$ , and output  $y_t \in \mathbb{R}^{n_y}$  evolve as follows,

$$\begin{cases} x_{t+1} = Ax_t + Bu_t + \epsilon_t \\ y_t = Cx_t + \nu_t, \end{cases} \quad (1)$$

where  $\epsilon_t \in \mathbb{R}^{n_x}$  is process noise and  $\nu_t \in \mathbb{R}^{n_y}$  is measurement noise.

The output at time  $t$  of the system in Equation (1) can be expressed as follows:

$$y_t = C \left( A^t x_0 + \sum_{i=1}^t A^{t-i} (B u_i + \epsilon_i) \right) + \nu_t \quad (2)$$

**Problem Statement:** Given a set of demonstrations, where only the output sequence  $\{y_\tau\}_{\tau \in [T]}$  is measured, and a model of the system, the goal is to find a reactive policy  $\Pi(\cdot)$  that matches the performance of the one used in these demonstrations, i.e., a policy is a mapping that satisfies,  $u_t = \Pi(y_t)$ .

In order to do so, as an intermediate goal, we wish to estimate the inputs of the system from the given demonstrations. Then we will use these (estimated) input-output pairs as training examples for a supervised learning algorithm in order to learn a policy  $\Pi(\cdot)$ .

The two step algorithm is a key aspect of the algorithm. For the first step, we can use all measurements  $\{y_\tau\}_{\tau \in [T]}$  to predict  $\hat{u}_t \approx u_t$ , and in the second step we use only the current time step measurement  $y_t$  to learn the policy,  $\hat{u}_t \approx \Pi(y_t)$ .

## Assumptions

Here we present the assumptions that we make throughout this paper.

**Input functions.** We will consider the inputs  $u_t$  to be a function of the time step  $t$  and the output  $y_t$ , i.e.,  $u_t = f(t, y_t)$ . This models both a trajectory following input as well as a closed-loop output feedback controller. As we will discuss later, this model also allows to account for model mismatches when the true model is not exactly known.

**Assumption 1.** *The input function  $f(\cdot)$  is a Lipschitz continuous function: For any  $(t_1, t_2) \in \mathbb{R}$  it holds that  $\|u_{t_1} - u_{t_2}\|_2 = \|f(t_1, y_{t_1}) - f(t_2, y_{t_2})\| \leq L \cdot (d_\tau(t_1, t_2) + d_y(y_{t_1}, y_{t_2}))$ , where the distance function  $d(\cdot, \cdot)$  is set and known in advance.*

**Assumption 2.** *The process  $\epsilon_t$  and measurement  $\nu_t$  noise sequences are independent and identically distributed with zero-mean and bounded support. That is, for any  $t \in [1, \dots, T]$  it holds that  $\mathbb{E}[\epsilon_t] = \mathbb{E}[\nu_t] = 0$ , and  $|\epsilon_t| \leq b_\epsilon$  and  $|\nu_t| \leq b_\nu$ , for some given  $b_\epsilon > 0$  and  $b_\nu > 0$ .*

**Assumption 3.** *The initial state  $x_0$  is unknown. However, we will consider that we have an unbiased estimate of the initial state, denoted by  $\hat{x}_0$ , hence  $x_0 \equiv \hat{x}_0 + \epsilon_0$ .*

**Assumption 4.** *The system  $(A, B, C)$  is perfectly known.*

**Assumption 5.** *The matrix  $H_\tau \equiv \sum_{i=0}^{\tau-1} A^i$  is invertible for all  $\tau \in [T]$ .*

**Remark 1.** Assumption 1 is rather standard in dynamical systems and is a sufficient condition for uniqueness of the state and output trajectories. In our work, we use  $d_\tau(t_1, t_2) = |t_2 - t_1|$  and  $d_y(y_{t_1}, y_{t_2}) = \|y_{t_2} - y_{t_1}\|_2$ . We need Assumption 2 to apply Hoeffding's inequality when deriving an upper bound for the estimation error. Alternatively, we could assume that

the variance is bounded and apply Bernstein inequalities. The results and analysis remain qualitatively similar. Assumptions 3 and 4 will be relaxed after deriving the estimator. These relaxations introduce an extra bias in the estimator that does not reduce help to reduce its variance. However, this is inherent to real-world systems and it is important to understand the errors they introduce in our estimator.

Finally, Assumption 5 is in most cases satisfied. The eigenvalues of the matrix  $H_\tau$  are  $1 + \lambda + \lambda^2 + \dots + \lambda^{\tau-1}$ , where  $\lambda$  is an eigenvalue of  $A$ . The eigenvalues could be zero if  $\lambda$  is in the complex unit circle (except for  $\lambda = 1$ ). If the system has friction, or it is unstable, then there are no eigenvalues in the unit circle and  $H_\tau$  is invertible.

### 3 Unsupervised Imitation Learning Algorithm

To implement the unsupervised imitation learning objective, we divide the problem into two steps: input estimation and unsupervised learning. For the former, the goal is to estimate a sequence of inputs  $\hat{u}_{1:T} \approx u_{1:T}$  given a sequence of outputs  $y_{1:T}$  and repeat this for each demonstration. For the latter, the objective is to find a policy,  $\Pi(\cdot)$ , that maps the outputs to the inputs at each time step  $\hat{u}_t \approx \Pi(y_t)$ . The whole approach is depicted in Algorithm 1.

---

**Algorithm 1:** Unsupervised Imitation Learning

---

**Data:** Outputs of  $N$  different demonstrations of length  $T$ ,  $\{y_{1:T}^i\}_{i=1}^N$ . System model  $(A, B, C)$ .

**Result:** Policy  $\Pi(\cdot)$ .

```

1  $D = \emptyset$ ;
2 for  $i = 1$  to  $N$  do
3    $\hat{u}_{1:T}^i \leftarrow \text{InputEstimation}(y_{1:T}^i, (A, B, C))$ ;
4   for  $t = 1$  to  $T$  do
5      $D = D \cup \{(y_t^i, \hat{u}_t^i)\}$ ;
6   end
7 end
8  $\Pi(\cdot) \leftarrow \text{ImitationLearning}(D, (A, B, C))$ 
```

---

The selection of the InputEstimation algorithm and the ImitationLearning algorithm are critical for the success of this approach. In this work, we used a behavioral cloning algorithm (vanilla supervised learning) for the imitation learning and we focus on the input estimation algorithm.

The UMV-IE (unbiased minimum-variance input estimator) of Gillijns and De Moor [2007] is the natural candidate for input estimation, since it is widely used in the control community. Unfortunately, upon using this estimator we have failed to learn stable policies, as can be observed in Table 2 in the Experiments section. The intuition behind this is that the input signal has the same magnitude as the noise that perturbs the system outside of the equilibrium in the demonstrations. As the UMV-IE estimates  $\hat{u}_t$  have high variance due to the unbiasedness constraints, the supervised learning algorithm with this data fails to learn a successful policy. Based on this observation, we develop an algorithm, called Adaptive-Linear

input estimator (AdaL-IE) that explicitly trades-off bias for variance to reduce the total estimation error. We will use AdaL-IE in line 3 of Algorithm 1 and evaluate its performance in Section 5.2. The next section discusses AdaL-IE.

## 4 Adaptive Linear Input Estimator

In this section, we find an estimate of the sequence of inputs  $\hat{u}_{1:T} \approx u_{1:T}$  given the measurements  $y_{1:T}$ , and a model of the system. We will decompose this problem into  $T$  problems: for each  $t = 1, \dots, T$ , we find a function that maps the measurements to an estimate of the input  $\hat{u}_t = \Psi_t(y_{1:T}) \approx u_t$ . The derivation of the estimator will be done for system of the form  $(A, I, I)$  where every input affects a state and all states are measured ( $B = I, C = I$ ). Though restrictive, this will help to understand the intuition behind the estimator and the parameters that affect it. Furthermore, in Section 4.3 this system will be relaxed to a more general non-linear system. The estimator,  $\Psi_t(\cdot)$ , adapts at every time step  $t$  to the measurements  $y_{1:T}$ , and it is a locally weighted average of the measurements  $y_{1:T}$ , hence the name Adaptive-Linear input estimator (AdaL-IE).

### 4.1 Estimator architecture

We search for an estimator that has a lower error than UMV-IE. For this, we relax the unbiasedness architecture and propose the following form:

$$\hat{u}_t = \sum_{\tau=1}^T \alpha_t[\tau] H_\tau^{-1} (y_\tau - A^\tau \hat{x}_0), \quad (3)$$

where the parameters  $\alpha_t$  are defined over the simplex,  $\Delta_T = \{\alpha_t \in \mathbb{R}^T \mid \sum_{\tau=1}^T \alpha_t[\tau] = 1 \text{ and } \alpha_t[\tau] \geq 0, \forall \tau \in \{1, 2, \dots, T\}\}$ . Given the above form for the estimator, our goal is to find the weight vector  $\alpha_t$  that minimizes the error between the true and estimated signal,  $\|u_t - \hat{u}_t\|$ .

Next we give some intuition behind the structure of the estimators that we consider in Equation (3). Let us define by  $U$  the vector that concatenates the whole input signals, i.e.,  $U = (u_1, \dots, u_T)$ . Now fixing  $t \in \{1, \dots, T\}$ , we can decompose  $U$  into two signals  $U_1, U_2$  as follows,

$$U = U_1 + U_2 := (u_t, u_t, \dots, u_t) + (u_1 - u_t, u_2 - u_t, \dots, u_T - u_t) .$$

i.e.,  $U_1$  is a signal such that in each step is exactly the input  $u_t$ , and  $U_2 = U - U_1$ . By linearity, the output of the system is the sum of the outputs of the two inputs. It is immediate to show that the  $U_1$  signal generates the following output signal,

$$y_\tau^{(1)} = A^\tau \hat{x}_0 + H_\tau u_t, \quad \forall \tau \in \{1, \dots, T\}$$

while  $U_2$  compensates to generate the output expressed in Equation (2). It can be shown that given the (imaginary) output  $y_\tau^{(1)}$  one can compute  $u_t$  as follows,

$$u_t = H_\tau^{-1} (y_\tau^{(1)} - A^\tau \hat{x}_0) .$$

As the above holds for any  $\tau \in \{1, \dots, T\}$  one can take any wighted average of the above estimators, i.e., for any  $\alpha \in \Delta$ , we can estimate,

$$u_t = \sum_{\tau=1}^T \alpha[\tau] H_\tau^{-1} (y_\tau^{(1)} - A^\tau \hat{x}_0) ,$$

which has the same form of Equation (3). Of course there is a challenge in choosing the weight vector due to the fact that the above strictly holds only for the (imaginary) output sequence  $\{y_\tau^{(1)}\}_\tau$  rather than the true output  $\{y_\tau\}_\tau$ . As we show next our choice of the weights directly balances a bias-variance tradeoff. We further comment that the estimator that we propose resembles in spirit to the weighted nearest neighbor (NN) estimator [Anava and Levy, 2016, Cover and Hart, 1967].

## 4.2 Optimization Problem

Given the estimator architecture, our goal is to find the best coefficients  $\alpha_t$ , that minimize the squared 2-norm of the estimation error

$$\min_{\alpha_t \in \Delta_T} \left\| \sum_{\tau=1}^T \alpha_t[\tau] H_\tau^{-1} (y_\tau - A^\tau \hat{x}_0) - u_t \right\|^2 \quad (4)$$

Although this problem is convex on  $\alpha_t$  and looks like a typical regression problem, we do not have the targets  $u_t$ . To bypass this problem, we base ourselves in the analysis of Anava and Levy [2016] and decompose our objective in Equation (4) into bias and variance terms to find a relaxed objective:

$$\begin{aligned} \left\| \sum_{\tau=1}^T \alpha_t[\tau] H_\tau^{-1} (y_\tau - A^\tau \hat{x}_0) - u_t \right\|^2 &= \left\| \sum_{\tau=1}^T \alpha_t[\tau] H_\tau^{-1} \left( A^\tau \epsilon_0 + \sum_{i=1}^{\tau} A^{\tau-i} (u_i + \epsilon_i) \right) + \nu_\tau - u_t \right\|^2 \\ &\leq \underbrace{2 \left\| \sum_{\tau=1}^T \alpha_t[\tau] H_\tau^{-1} \left( \sum_{i=0}^{\tau} A^{\tau-i} \epsilon_i + \nu_\tau \right) \right\|^2}_{\text{variance}} + \underbrace{2 \left\| \sum_{\tau=1}^T \alpha_t[\tau] H_\tau^{-1} \left( \sum_{i=1}^{\tau} A^{\tau-i} (u_i - u_t) \right) \right\|^2}_{\text{bias}^2} \end{aligned}$$

Furthermore, the bias term can be bounded as follows:

$$\text{bias} = \left\| \sum_{\tau=1}^T \alpha_t[\tau] H_\tau^{-1} \left( \sum_{i=1}^{\tau} A^{\tau-i} (u_i - u_t) \right) \right\| \leq L \alpha_t^\top q_t,$$



where  $q_t \in \mathbb{R}^T$  is a vector that depends on the system dynamics and the distance metric between the index and the desired step to predict  $t$ , as well as of  $L$ , the Lipschitz constant of the input function.

Finally, using Hoeffding's inequality for matrix concentrations [Juditsky and Nemirovski, 2008, Kakade], the variance term can be bounded with probability  $(1 - \delta)$  as follows:

$$\text{var} = \left\| \sum_{\tau=1}^T \alpha_t[\tau] H_\tau^{-1} \left( \sum_{i=0}^{\tau} A^{\tau-i} \epsilon_i + \nu_\tau \right) \right\|^2 \leq V \left( 1 + \sqrt{\log(\delta^{-1})} \right)^2 \alpha_t^\top Q \alpha_t$$

where  $Q \in \mathbb{R}^{T \times T}$  is a strictly positive definite matrix that depends on the system dynamics, and  $V$  is a positive constant that depends on the noise level.

**Proposition 2.** *The optimization problem in Equation (4) can be upper bounded with probability  $1 - \delta$  by*

$$\min_{\alpha_t \in \Delta_n} 2L^2 \alpha_t^\top \left( \frac{V}{L^2} \left( 1 + \sqrt{\log(\delta^{-1})} \right)^2 Q + q_t q_t^\top \right) \alpha_t \quad (5)$$

*Proof.* In Appendix A. □

The relaxed optimization problem Equation (5) is a quadratic program over the simplex, and its parameters depend on the system dynamics, the signal to noise ratio  $\frac{V}{L^2}$ , the distance metric used, and the confidence level used when bounding the variance. The multiplicative factor  $2L^2$  does not affect the optimal solution. The matrix  $Q$  is strictly positive definite and the matrix  $q_t q_t^\top$  is positive semi-definite matrix, hence the function to optimize is strictly convex and the solution is unique. This solution can be efficiently computed via projected gradient descent [Boyd and Vandenberghe, 2004]. The solution  $\alpha_t^*$  will be different for every estimation point  $\hat{u}_t$  as the bias term  $q_t$  depends on the distance  $d(t, \cdot) = d_\tau(t, \cdot) + d_y(y_t, \cdot)$ .

The optimal solution of Equation (5) is used in Equation (3) to estimate the input. As in Anava and Levy [2016], we expect the solution to have a limited support concentrated around  $t$ . This is since the further away the indexes  $\tau$  are from the estimation point  $t$ , the larger  $q_t[\tau]$ . Which in turn implies that  $\alpha_t[\tau]$  should decay when  $\tau$  is further away from  $t$ . This limited support of the optimal weights is observed in our experiments: as we show in Figure 2 only a small number of indexes around  $t$  have non-zero entries.

**System Mismatch** If the true system matrix  $A$  has a mismatch with the estimates  $\hat{A}$ , i.e.  $A = \hat{A} + \Delta_A$  then the system can be expressed as:

$$\begin{cases} x_{t+1} = Ax_t + u_t + \epsilon_t = \hat{A}x_t + (\Delta_A x_t + u_t) + \epsilon_t \\ y_t = x_t + \nu_t, \end{cases}$$

By renaming  $\tilde{u}_t = \Delta_A x_t + u_t$  then the same analysis can be used to recover  $\tilde{u}_t$ . The Lipschitz constant of  $\tilde{u}$  is  $\tilde{L} = \|\Delta_A\| + L$ . If the mismatch is too big, then  $\|\Delta_A\|$  dominates the signal information of  $u_t$  and the upper bound of the bias becomes too loose.



**Initial State knowledge** If the initial state of the system is unknown, then the estimation will have an extra bias of  $\sum_{\tau=1}^T \alpha_t[\tau] H_\tau^{-1} A^\tau \hat{x}_0$ . For estimating inputs at time  $t$  close to 0, this term is significant. However, if the system is stable, as time  $t$  increases, this term goes to zero. If the system is unstable, the bias that arises is  $A_{US} \hat{x}_0$ , where  $A_{US}$  are the unstable modes of  $A$ .

### 4.3 Extensions to non-linear and time varying dynamical systems

In this section we extend the input estimator AdaL-IE to a very general class of non-linear systems which include most robotics systems [Theodorou et al., 2010]. These systems are of the form:

$$\begin{cases} x_{t+1} = g(x_t) + h(x_t)u_t + \epsilon_t \\ y_t = o(x_t) + \nu_t, \end{cases}$$

where  $g(x_t)$ ,  $h(x_t)$ , and  $o(x_t)$  are non-linearities that depend only on the current state. Up to second order errors, the system is equivalent to a time-varying system:

$$\begin{cases} x_{t+1} = A_t x_t + B_t u_t + \epsilon_t \\ y_t = C_t x_t + \nu_t, \end{cases}$$

where  $A_t = \frac{\partial g(x)}{\partial x} \Big|_{x=x_t}$ ,  $B_t = h(x_t) + \frac{\partial h(x)}{\partial x} x \Big|_{x=x_t}$ , and  $C_t = \frac{\partial o(x)}{\partial x} \Big|_{x=x_t}$ . The successive systems are found by linearizing the non-linear systems around the state trajectory.

**Assumption 6.** *The row span of matrix  $C_t$  is equal to the number of states, for all  $t$ .*

Using this assumption the condition  $C_t^\dagger C_t = I$  is satisfied. Next, we can define the input  $\tilde{u}_t \equiv B_t u_t$  and recover an estimate of  $\hat{\tilde{u}}_t = B_t \hat{u}_t$ . From this estimate, the best estimate of the original input (in terms of the minimum 2-norm) is given by  $\hat{u}_t = B_t^\dagger \hat{\tilde{u}}_t$ . Finally, let's define the matrices  $\Phi(t, i) = A_{t-1} \Phi(t-1, i)$ , for  $0 \leq i < t$ , and  $\Phi(t, i) = I$ , for  $i = t$ . With a slight abuse of notation, we rename  $H_\tau = \sum_{i=1}^\tau \Phi(\tau, i)$ . The estimator becomes:

$$\hat{u}_t = B_t^\dagger \left( \sum_{\tau=1}^T \alpha_t[\tau] H_\tau^{-1} C_\tau^\dagger (y_\tau - \Phi(\tau, 0) \hat{x}_0) \right). \quad (6)$$

The optimization problem to find  $\alpha_t^*[\tau]$  is a straight forward generalization of Proposition 2.

## 5 Experiments

### 5.1 Input Estimation.

We performed a set of experiments to evaluate the input estimator and compared the RMS error of it with the benchmark [Gillijns and De Moor, 2007]. We applied a set of 8 different input signals to 5 different system for 20 episodes of 100 time-steps. Even though the input

signals were a priori known, we fit the SNR ratio needed for setting up the optimization problem in Equation (5) via cross-validation. To simulate modeling mismatch, we perturbed the entries of the state transition matrix of each system with Gaussian noise. The signals were (a) a unit step, (b) a unit sine, (c) a unit ramp, (d) a unit triangle, (e) a ramp followed by a unit step, (f) a ramp followed by a zero step, (g) a unit step followed by a zero step, and (h) a unit sine superposed to a unit step. The systems were (1) a spring-mass system, (2) a double integrator, (3) a email server [Hellerstein et al., 2004, Section 2.6.1], (4) a HTTP server [Hellerstein et al., 2004, Section 7.8.1], (5) a stable system with random coefficients in the state transition matrix, (6) a first order non-linear system [Khalil, 2002, Example 4.27], and (7) a second order non-linear system [Khalil, 2002, Example 4.61].

The estimation signals of system (1) are shown in Figure 1 and the mean RMS errors are shown in Table 1. The estimations on other systems and the full table with standard deviations are deferred to Appendix B. In each of the sub-figures, we plot the input signal in blue, in shaded green, the UMV-IE estimates mean plus/minus one standard deviation, and in shaded red, the analogous results from AdaL-IE. In all cases, AdaL-IE estimates have much lower variance than UMV-IE estimates, but at the cost of some bias. From the 56 experiments, in 50 AdaL-IE outperforms UMV-IE, while UMV-IE only outperforms AdaL-IE in 3.

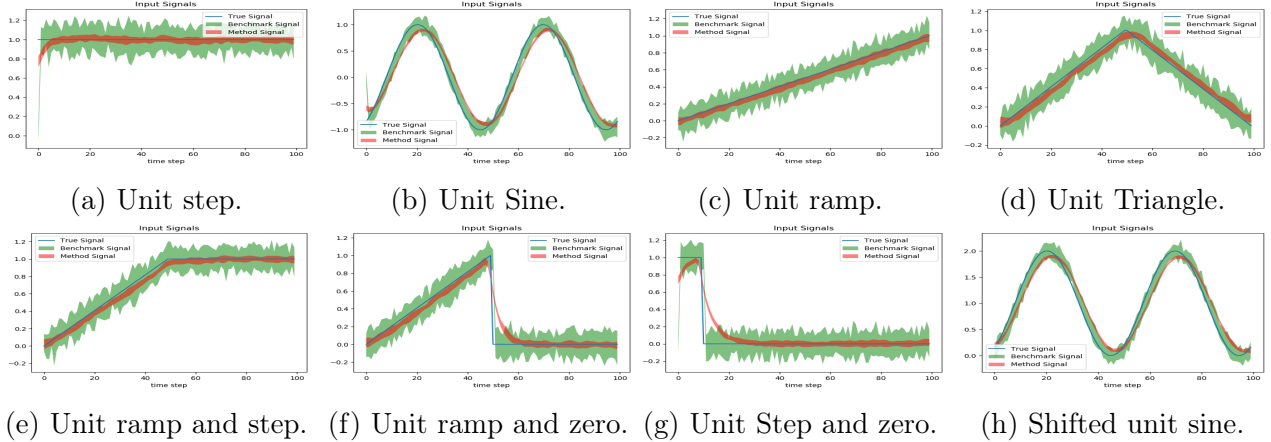


Figure 1: Input signal estimations on double integrator system.

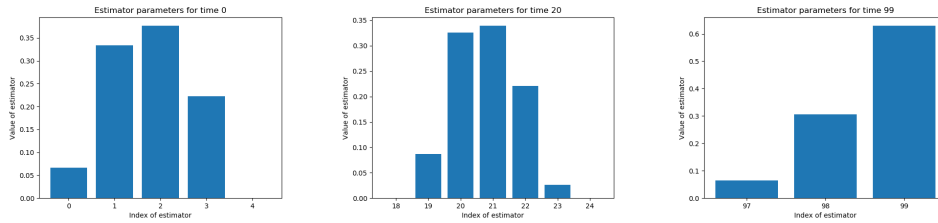
A particular effect happens in signals where the input signal changes abruptly, such as (f) and (g). The input function is defined over two domains, each of these Lipschitz continuous. However, at the discontinuity point, assumption 1 is violated or the constant  $L \rightarrow \infty$ . Thus, learning a global Lipschitz constant by cross-correlation introduces this delay. A possible solution for this is using a Lipschitz constant  $L_j$  for each time step  $j$ . Where the function does not change much,  $L_j$  is small, and where the function has big changes,  $L_j$  is large. When  $L_j$  is big, then the bias term is big as well, and the optimization problem decreases the support of  $\alpha_t$ . At the discontinuity point, the estimate would have a higher variance, but a lower bias.

Table 1: In each cell indexed by a combination signal/system, we show the mean RMS error. Within each cell, the top row shows the mean RMS error of AdaL-IE and the bottom method of UMV-IE.

	Spring-mass	Double integrator	Email server	HTTP server	Random system	Non-linear 4.27	Non-Linear 4.61
(a)	<b>0.061</b> 0.191	<b>0.049</b> 0.187	<b>0.112</b> 0.325	<b>0.234</b> 0.885	<b>0.049</b> 0.188	<b>0.237</b> 1.673	<b>0.237</b> 1.673
(b)	<b>0.544</b> 1.626	0.194 0.202	<b>0.139</b> 0.334	<b>0.318</b> 0.887	0.375 <b>0.228</b>	<b>0.500</b> 1.678	<b>0.500</b> 1.677
(c)	<b>0.584</b> 1.666	<b>0.044</b> 0.162	<b>0.123</b> 0.317	<b>0.241</b> 0.898	<b>0.085</b> 0.166	<b>0.257</b> 1.674	<b>0.263</b> 1.677
(d)	<b>0.063</b> 0.162	<b>0.055</b> 0.162	<b>0.113</b> 0.310	<b>0.255</b> 0.869	<b>0.056</b> 0.161	<b>0.285</b> 1.677	<b>0.259</b> 1.681
(e)	0.073 <b>0.021</b>	<b>0.049</b> 0.161	<b>0.111</b> 0.312	<b>0.239</b> 0.859	<b>0.062</b> 0.156	<b>0.261</b> 1.681	<b>0.266</b> 1.645
(f)	<b>0.584</b> 1.640	<b>0.102</b> 0.187	<b>0.131</b> 0.320	<b>0.267</b> 0.889	<b>0.163</b> 0.221	<b>0.297</b> 1.653	<b>0.307</b> 1.650
(g)	<b>0.123</b> 0.217	<b>0.120</b> 0.217	<b>0.137</b> 0.345	<b>0.274</b> 0.910	0.259 0.277	<b>0.290</b> 1.651	<b>0.294</b> 1.676
(h)	<b>0.579</b> 1.638	0.176 0.183	<b>0.140</b> 0.324	<b>0.305</b> 0.897	0.533 <b>0.222</b>	<b>0.533</b> 1.676	<b>0.515</b> 1.701

**Sparsity of estimator parameters.** The solution of the optimization problem in Equation (5) has a very special sparsity pattern as shown in the sub-figures Figures 2a to 2c. Figure 2a and Figure 2c show the estimators at both ends of the horizon, showing the so-called *end effects* on the parameters. The rest of the estimators have a very similar pattern to those of sub-figure Figure 2b. For estimating input 20, only outputs between time 19 and 23 are non-zero. This coincides with the intuition that input at time 20 will only affect current and future outputs. However, input 19 is close to input 20 because of the Lipschitz continuity assumption, hence output 19 also has some information about input at time 20.

The sparsity pattern is induced by the bias term. The further away an output is from the estimated input, the higher the bias. Thus, the cost of including these non-zero weights is larger than the reduction in variance due to averaging. This observation was also noted in Anava and Levy [2016].



(a) Parameters at  $t = 0$ . (b) Parameters at  $t = 20$ . (c) Parameters at  $t = 99$ .

Figure 2: Sparsity pattern and non-zero parameters of estimator.

**Noise Magnitude Effect.** To understand the trade-off between bias and variance that the estimator has, we analyzed the spring-mass system with three different magnitudes of noise variances. We show the results in Figure 3. When the noise variance is small compared to the

magnitude of the signal as in Figure 3a, then the bias is larger than the variance reduction and the benchmark performs better. On the other hand, when the noise variance has the same magnitude as the signal, then the bias is meaningless as shown in Figure 3c. Even for cases in which the noise is smaller than the signal, the variance reduction is comparable as shown in Table 1.

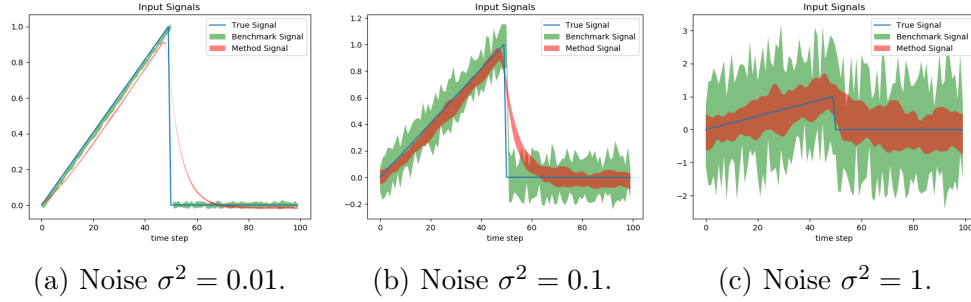


Figure 3: Estimator performance with different noise magnitudes.

## 5.2 Unsupervised policy learning.

After analyzing the quality of the data that the estimator recovers, the question that we analyze in this section is if this data is *good enough* to learn a policy that successfully executes a given task. As a benchmark, we considered the swing up pendulum task of openAI gym [Brockman et al., 2016]. The policy used to generate *teacher* trajectories was a feedback linearizing controller,  $f(\phi, \omega) = 15 \sin(\phi) + 30\phi + 8\omega$ , where  $\phi$  is the angular position and  $\omega$  the angular velocity of the pendulum. Additively to the input created by the policy, we simulated process and measurement noise. A task is considered successful if the policy stabilizes the pendulum in the upright position after 100 seconds.

We followed Algorithm 1 to learn the policy. We used both AdaL-IE and UMV-IE for the input estimator and vanilla supervised learning for the imitation learning algorithm. We experimented with 3 different architectures, a linear function that mapped the measurements to the outputs, a neural network with 2 hidden layers of 5 neurons with ReLU activation layers, and a neural network with the same architecture but sigmoid activation layers.

The original controller stabilizes the system 930 out of 1000 test cases from random initial conditions. We show the experimental results in Table 2. For the linear architecture, the controller learned using the input recovered with AdaL-IE stabilizes (theoretically) the linearized system around the unstable equilibrium, while the controller learned using the benchmark method to estimate inputs does not, hence is never able to stabilize the system. The policy stabilizes only 496 out of 1000 experimental runs with this controller because the learned controller fails to account for the non-linearities that the real controller has. When exploring different architectures the Sigmoid activation functions perform better than the linear because it has more representational power and can fit better the original controller. On the other hand, the architecture with ReLU activations performs worst because it has

very sharp boundaries. Inspecting the experiments with ReLU activation functions, the policy tries to stabilize near the equilibrium but small perturbations in the measurement generate big changes in the outputs of the controller and this drives the system to instability.

Table 2: Successfully learned controllers.

Controller	AdaL-IE Targets	UMV-IE Targets
Linear Architecture	496	0
ReLU Activations	332	0
Sigmoid Activations	754	224

## 6 Conclusion

In this paper, we presented two contributions: a new input estimator for a general class of dynamical systems and the novel idea of using this as a first step in an imitation learning pipeline. We presented an upper bound on the estimation error and showed its performance with experiments.

An interesting final observation is that this method can be implemented even without any demonstration. The sequence  $y_{1:T}$  can be any imagined physically feasible trajectory. Using AdaL-IE, we estimate a sequence of inputs  $u_{1:T}$  that produce this sequence. Applying this sequence open loop can produce arbitrarily bad trajectories due to system mismatch, noise, and non-linearities. Instead, we use imitation learning to fit a policy that predicts  $u_t = \Pi(y_t)$  and deploy this policy.

## Acknowledgements

K.Y.L. is supported by the ETH Zurich Postdoctoral Fellowship and Marie Curie Actions for People COFUND program.

## References

- P. Abbeel and A. Y. Ng. Apprenticeship learning via inverse reinforcement learning. In *Proceedings of the twenty-first international conference on Machine learning*, page 1. ACM, 2004.
- G. Anagnostou and B. C. Pal. Derivative-free kalman filtering based approaches to dynamic state estimation for power systems with unknown inputs. *IEEE Transactions on Power Systems*, 33(1):116–130, 2018.
- O. Anava and K. Levy. k\*-nearest neighbors: From global to local. In *Advances in Neural Information Processing Systems*, pages 4916–4924, 2016.

- B. D. Argall, S. Chernova, M. Veloso, and B. Browning. A survey of robot learning from demonstration. *Robotics and autonomous systems*, 57(5):469–483, 2009.
- A. Billard, S. Calinon, R. Dillmann, and S. Schaal. Robot programming by demonstration. In *Springer handbook of robotics*, pages 1371–1394. Springer, 2008.
- M. Bojarski, D. Del Testa, D. Dworakowski, B. Firner, B. Flepp, P. Goyal, L. D. Jackel, M. Monfort, U. Muller, J. Zhang, et al. End to end learning for self-driving cars. *arXiv preprint arXiv:1604.07316*, 2016.
- L. Bolliger, H.-A. Loeliger, and C. Vogel. Lmmse estimation and interpolation of continuous-time signals from discrete-time samples using factor graphs. *arXiv preprint arXiv:1301.4793*, 2013.
- S. Boyd and L. Vandenberghe. *Convex optimization*. Cambridge university press, 2004.
- G. Brockman, V. Cheung, L. Pettersson, J. Schneider, J. Schulman, J. Tang, and W. Zaremba. Openai gym. *arXiv preprint arXiv:1606.01540*, 2016.
- M. Corless and J. Tu. State and input estimation for a class of uncertain systems. *Automatica*, 34(6):757–764, 1998.
- T. Cover and P. Hart. Nearest neighbor pattern classification. *IEEE transactions on information theory*, 13(1):21–27, 1967.
- A. D. Edwards, H. Sahni, Y. Schroeker, and C. L. Isbell. Imitating latent policies from observation. *arXiv preprint arXiv:1805.07914*, 2018.
- G. F. Franklin, J. D. Powell, and M. L. Workman. *Digital control of dynamic systems*, volume 3. Addison-wesley Menlo Park, CA, 1998.
- S. Gillijns and B. De Moor. Unbiased minimum-variance input and state estimation for linear discrete-time systems. *Automatica*, 43(1):111–116, 2007.
- F. Girardin, D. Remond, and J.-F. Rigal. High frequency correction of dynamometer for cutting force observation in milling. *Journal of Manufacturing Science and engineering*, 132(3):031002, 2010.
- J. L. Hellerstein, Y. Diao, S. Parekh, and D. M. Tilbury. *Feedback control of computing systems*. John Wiley & Sons, 2004.
- A. Hussein, M. M. Gaber, E. Elyan, and C. Jayne. Imitation learning: A survey of learning methods. *ACM Computing Surveys (CSUR)*, 50(2):21, 2017.
- A. Juditsky and A. S. Nemirovski. Large deviations of vector-valued martingales in 2-smooth normed spaces. *arXiv preprint arXiv:0809.0813*, 2008.

- S. Kakade. Lecture notes in multivariate analysis, dimensionality reduction, and spectral methods. [http://stat.wharton.upenn.edu/~skakade/courses/stat991\\_mult/lectures/MatrixConcen\\_derivations.pdf](http://stat.wharton.upenn.edu/~skakade/courses/stat991_mult/lectures/MatrixConcen_derivations.pdf). April 2010.
- H. K. Khalil. Nonlinear systems, 3rd. *New Jersey, Prentice Hall*, 9(4.2), 2002.
- J. Kober, J. A. Bagnell, and J. Peters. Reinforcement learning in robotics: A survey. *The International Journal of Robotics Research*, 32(11):1238–1274, 2013.
- Y. Liu, A. Gupta, P. Abbeel, and S. Levine. Imitation from observation: Learning to imitate behaviors from raw video via context translation. *arXiv preprint arXiv:1707.03374*, 2017.
- K. Maes, S. Gillijns, and G. Lombaert. A smoothing algorithm for joint input-state estimation in structural dynamics. *Mechanical Systems and Signal Processing*, 98:292–309, 2018.
- S. S. Park and Y. Altintas. Dynamic compensation of spindle integrated force sensors with kalman filter. *Journal of Dynamic Systems, Measurement, and Control*, 126(3):443–452, 2004.
- S. Ross, G. Gordon, and D. Bagnell. A reduction of imitation learning and structured prediction to no-regret online learning. In *Proceedings of the fourteenth international conference on artificial intelligence and statistics*, pages 627–635, 2011.
- S. Schaal. Is imitation learning the route to humanoid robots? *Trends in cognitive sciences*, 3(6):233–242, 1999.
- E. Theodorou, J. Buchli, and S. Schaal. A generalized path integral control approach to reinforcement learning. *Journal of Machine Learning Research*, 11(Nov):3137–3181, 2010.
- F. Torabi, G. Warnell, and P. Stone. Behavioral cloning from observation. *arXiv preprint arXiv:1805.01954*, 2018.



## A Appendix: Proof of Proposition 2

For readability we will reproduce the Proposition 2 below:

**Proposition 2.** The optimization problem in Equation (4) can be upper bounded by

$$\min_{\alpha_t \in \Delta_n} 2L^2 \alpha_t^\top \left( \frac{V}{L^2} \left( 1 + \sqrt{\log(\delta^{-1})} \right)^2 Q + q_t q_t^\top \right) \alpha_t$$

*Proof.* We will proof the Proposition for the non-linear extension presented in Section 4.3. We start by renaming  $B_t u_t = \tilde{u}_t$ , then the error can be upper bounded as:

$$\begin{aligned} \text{error}^2 &= \left\| \sum_{\tau=1}^T \alpha_t[\tau] H_\tau^{-1} C_\tau^\dagger (y_\tau - \Phi(\tau, 0) \hat{x}_0) - \tilde{u}_t \right\|^2 \\ &= \left\| \sum_{\tau=1}^T \alpha_t[\tau] H_\tau^{-1} \left( \Phi(\tau, 0) \epsilon_0 + \sum_{i=1}^{\tau} \Phi(\tau, i) (\tilde{u}_i + \epsilon_i) \right) + \nu_t \right\|^2 \\ &= \left\| \sum_{\tau=1}^T \alpha_t[\tau] H_\tau^{-1} \left( \Phi(\tau, 0) \epsilon_0 + \sum_{i=1}^{\tau} \Phi(\tau, i) (\tilde{u}_i - \tilde{u}_t + \tilde{u}_t) + \epsilon_i \right) + \nu_t \right\|^2 \\ &= \left\| \sum_{\tau=1}^T \alpha_t[\tau] H_\tau^{-1} \left( \sum_{i=0}^{\tau} \Phi(\tau, i) \epsilon_i + \nu_t + \sum_{i=1}^{\tau} \Phi(\tau, i) (\tilde{u}_i - \tilde{u}_t) \right) \right\|^2 \\ &\leq \underbrace{2 \left\| \sum_{\tau=1}^T \alpha_t[\tau] H_\tau^{-1} \left( \sum_{i=0}^{\tau} \Phi(\tau, i) \epsilon_i + \nu_t \right) \right\|^2}_{\text{variance}} + \underbrace{2 \left\| \sum_{\tau=1}^T \alpha_t[\tau] H_\tau^{-1} \left( \sum_{i=1}^{\tau} \Phi(\tau, i) (\tilde{u}_i - \tilde{u}_t) \right) \right\|^2}_{\text{bias}^2} \end{aligned}$$

The bias term can be bounded as:

$$\begin{aligned} \text{bias} &= \left\| \sum_{\tau=1}^T \alpha_t[\tau] H_\tau^{-1} \left( \sum_{i=1}^{\tau} \Phi(\tau, i) (\tilde{u}_i - \tilde{u}_t) \right) \right\| \\ &= \left\| \sum_{\tau=1}^T \alpha_t[\tau] \left( \sum_{i=1}^{\tau} H_\tau^{-1} \Phi(\tau, i) (\tilde{u}_i - \tilde{u}_t) \right) \right\| \\ &\leq \sum_{\tau=1}^T |\alpha_t[\tau]| \left( \sum_{i=1}^{\tau} \|H_\tau^{-1} \Phi(\tau, i)\| \|\tilde{u}_i - \tilde{u}_t\| \right) \\ &\leq L \sum_{\tau=1}^T \alpha_t[\tau] \left( \sum_{i=1}^{\tau} \tilde{d}(i, t) \|H_\tau^{-1} \Phi(\tau, i)\| \right) \\ &= L \alpha_t^\top q_t, \end{aligned}$$

where  $\tilde{d}(i, t) = (\max_{j=\{i, t\}} \|B_j\|) d(i, t)$ . The first inequality comes from the triangular inequality and the second inequality comes from Lipschitz continuity of the input function given by Assumption 1. The  $\tau$ -th index of  $q_t$  is:

$$q_t[\tau] = \left( \sum_{i=1}^{\tau} \tilde{d}(i, t) \|H_{\tau}^{-1} \Phi(\tau, i)\| \right) \quad (7)$$

Finally, the variance term can be bounded using Hoeffding's inequality on matrix concentrations [Juditsky and Nemirovski \[2008\]](#), [Kakade](#) with high probability as:

$$\begin{aligned} \text{var} &= \left\| \sum_{\tau=1}^T \alpha_t[\tau] H_{\tau}^{-1} \left( \sum_{i=0}^{\tau} \Phi(\tau, i) \epsilon_i + \nu_t \right) \right\|^2 \\ &= \left\| \sum_{i=0}^T \left( \sum_{\tau=\max\{1, i\}}^T \alpha_t[\tau] H_{\tau}^{-1} \Phi(\tau, i) \right) \epsilon_i + \sum_{\tau=1}^T (\alpha_t[\tau] H_{\tau}^{-1}) \nu_t \right\|^2 \\ &= \left\| \sum_{i=0}^T E_i \epsilon_i + \sum_{\tau=1}^T N_t \nu_t \right\|^2 \\ &\leq 36 \sum_{i=0}^{2T} M_i^2 \left( 1 + \sqrt{\log(\delta^{-1})} \right)^2 \end{aligned}$$

where  $E_i = \sum_{\tau=\max\{1, i\}}^T \alpha_t[\tau] H_{\tau}^{-1} \Phi(\tau, i)$ , and  $N_t = \alpha_t[\tau] H_{\tau}^{-1}$ . The bound holds for  $M_i \geq \|E_i \epsilon_i\|$  for  $i \in \{0, \dots, T\}$  and  $M_i \geq \|N_t \nu_t\|$  for  $i \in \{T+1, \dots, 2T\}$ ,  $t = i-1$ .

Using Assumption 2, noise magnitude is bounded by  $b$ , then defining  $V \equiv 36b^2$

$$\begin{aligned} \text{var} &\leq V \left( 1 + \sqrt{\log(\delta^{-1})} \right)^2 \left( \sum_{i=0}^T \left\| \sum_{\tau=\max\{1, i\}}^T \alpha_t[\tau] H_{\tau}^{-1} \Phi(\tau, i) \right\|^2 + \sum_{\tau=1}^T \|\alpha_t[\tau] H_{\tau}^{-1}\|^2 \right) \\ &= V \left( 1 + \sqrt{\log(\delta^{-1})} \right)^2 \alpha_t^{\top} Q \alpha_t \end{aligned}$$

The entry  $\tau, \tau'$  of  $Q$  is:

$$Q[\tau, \tau'] = \sum_{i=0}^{\min\{\tau, \tau'\}} \|H_{\tau}^{-1} \Phi(\tau, i)\| \|H_{\tau'}^{-1} \Phi(\tau', i)\| + \|H_{\tau}^{-1}\|^2 \mathbb{1}[\tau = \tau'], \quad (8)$$

where  $\mathbb{1}[\tau = \tau'] = 1$  if  $\tau = \tau'$  and 0 otherwise. The first terms come from the process noise that accumulate with the running index  $i$ , while the last term corresponds to the measurement noise that only depends on the current time.  $\square$

## B Appendix: Extended Experiments

**Spring Mass** The continuous time spring mass system dynamics is given by:  $m\ddot{x} + c\dot{x} + kx = u_t$ , where  $m$  is the mass,  $c$  a friction coefficient,  $k$  an elasticity coefficient, and  $x$  the position at time  $t$ . We used a system with  $m = 250$ ,  $c = 60$ , and  $k = 80$ . We discretized the system with  $\Delta t = 1$ . We show the estimation signals in Figure 4 and the RMS errors with confidence intervals in Table 3.

**Double Integrator** The double integrator is a spring-mass system without elasticity and friction constants. In experiments we added a small friction coefficient for numerical stability of the simulations. We show the estimation signals in Figure 5 and the RMS errors with confidence intervals in Table 4.

**Email Server** The email server [Hellerstein et al., 2004, Section 2.6.1] dynamics is given in discrete time by  $x_{t+1} = 0.43x_t + 0.47u_t$ , where  $x_t$  is the number of remote procedure calls being processed by the server, and  $u_t$  the maximum number of client connections. We show the estimation signals in Figure 6 and the RMS errors with confidence intervals in Table 5.

**HTTP Server** The HTTP server [Hellerstein et al., 2004, Section 7.8.1] dynamics is a second order system given by  $x1_{t+1} = 0.54x1_t - 0.11x2_t - 8.5u1_t + 0.44u2_t$  and  $x2_{t+1} = 0.026x1_t + 0.63x2_t + -0.25u1_t + 0.28u2_t$ , where  $x1$  is the cpu usage,  $x2$  is the memory usage,  $u1$  is how long an idle HTTP connection is held, and  $u2$  is the number of concurrent connections to the web Server. We show the estimation signals in Figure 7 and the RMS errors with confidence intervals in Table 6.

**Random State Transition** The random system is a second order system with state transtion matrix  $A = 0.7I + 0.1W$ , where  $I$  is the identity and entries of  $W_{i,j}$  are normally distributed random variables. The input matrix is  $B = I$  and output matrix is  $C = I$ . We show the estimation signals in Figure 8 and the RMS errors with confidence intervals in Table 7.

**NonLinear System 1** This system from [Khalil, 2002, Example 4.27] has a dynamics given by:  $\dot{x}_1 = -x_1 + x_2^2$ ,  $\dot{x}_2 = -x_2 + u$ . We discretized the system with  $\Delta t = 0.1$ . We show the estimation signals in Figure 9 and the RMS errors with confidence intervals in Table 8.

**NonLinear System 2** This system from [Khalil, 2002, Example 4.61] has a dynamics given by:  $\dot{x}_1 = x_1 \left( \sin^2 \left( \frac{\pi x_2}{2} \right) - 1 \right)$ ,  $\dot{x}_2 = -x_2 + u$ . We discretized the system with  $\Delta t = 0.1$ . We show the estimation signals in Figure 10 and the RMS errors with confidence intervals in Table 9.

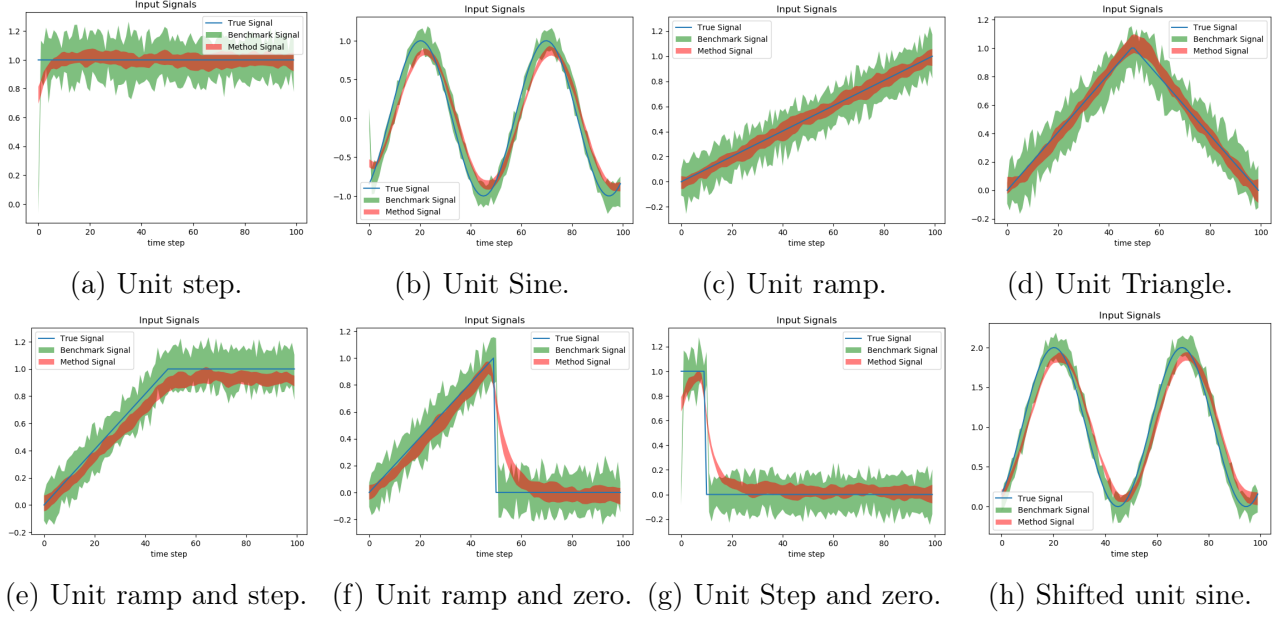


Figure 4: Input signal estimations on spring mass system.

Table 3: RMS error in input estimation on spring mass system

	(a)	(b)	(c)	(d)
AdaL-IE	<b><math>0.061 \pm 0.008</math></b>	<b><math>0.544 \pm 0.062</math></b>	<b><math>0.584 \pm 0.067</math></b>	<b><math>0.063 \pm 0.012</math></b>
UMV-IE	$0.191 \pm 0.012$	$1.626 \pm 0.101$	$1.666 \pm 0.120$	$0.162 \pm 0.011$
	(e)	(f)	(g)	(h)
AdaL-IE	$0.073 \pm 0.002$	<b><math>0.584 \pm 0.144</math></b>	<b><math>0.123 \pm 0.007</math></b>	<b><math>0.579 \pm 0.098</math></b>
UMV-IE	<b><math>0.021 \pm 0.001</math></b>	$1.640 \pm 0.087$	$0.217 \pm 0.012$	$1.638 \pm 0.125$

Table 4: RMS error in input estimation on double integrator system

	(a)	(b)	(c)	(d)
AdaL-IE	<b><math>0.049 \pm 0.008</math></b>	$0.194 \pm 0.010$	<b><math>0.044 \pm 0.005</math></b>	<b><math>0.055 \pm 0.008</math></b>
UMV-IE	$0.187 \pm 0.011$	$0.202 \pm 0.012$	$0.162 \pm 0.012$	$0.162 \pm 0.012$
	(e)	(f)	(g)	(h)
AdaL-IE	<b><math>0.049 \pm 0.008</math></b>	<b><math>0.102 \pm 0.006</math></b>	<b><math>0.120 \pm 0.006</math></b>	$0.176 \pm 0.011$
UMV-IE	$0.161 \pm 0.012$	$0.187 \pm 0.010$	$0.217 \pm 0.011$	$0.183 \pm 0.012$

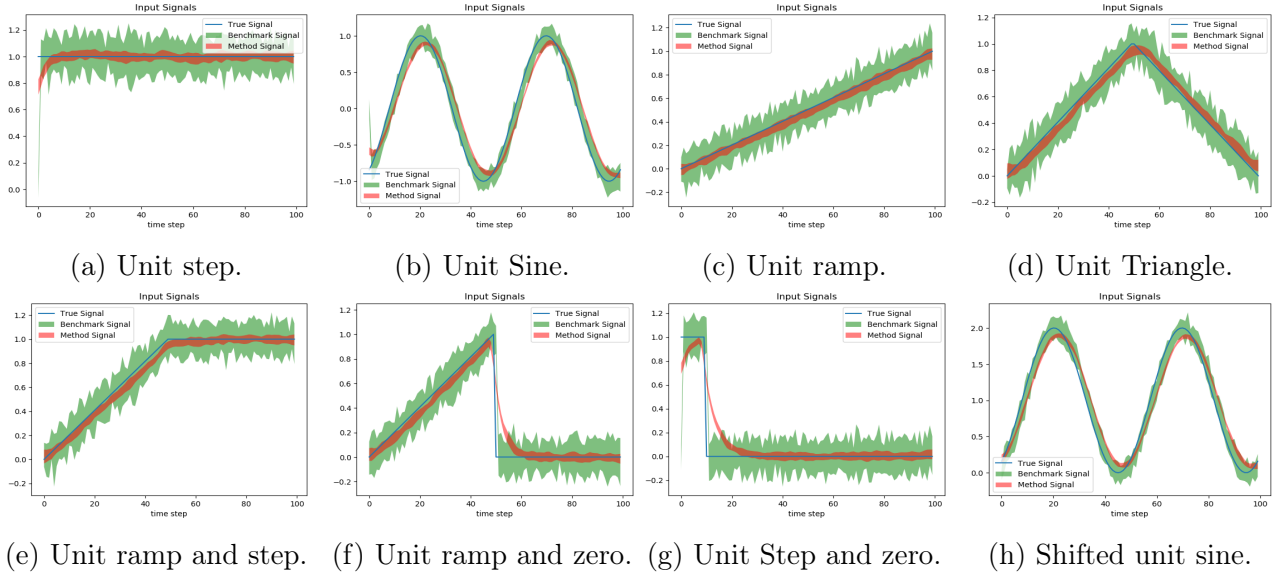


Figure 5: Input signal estimations on double integrator system.

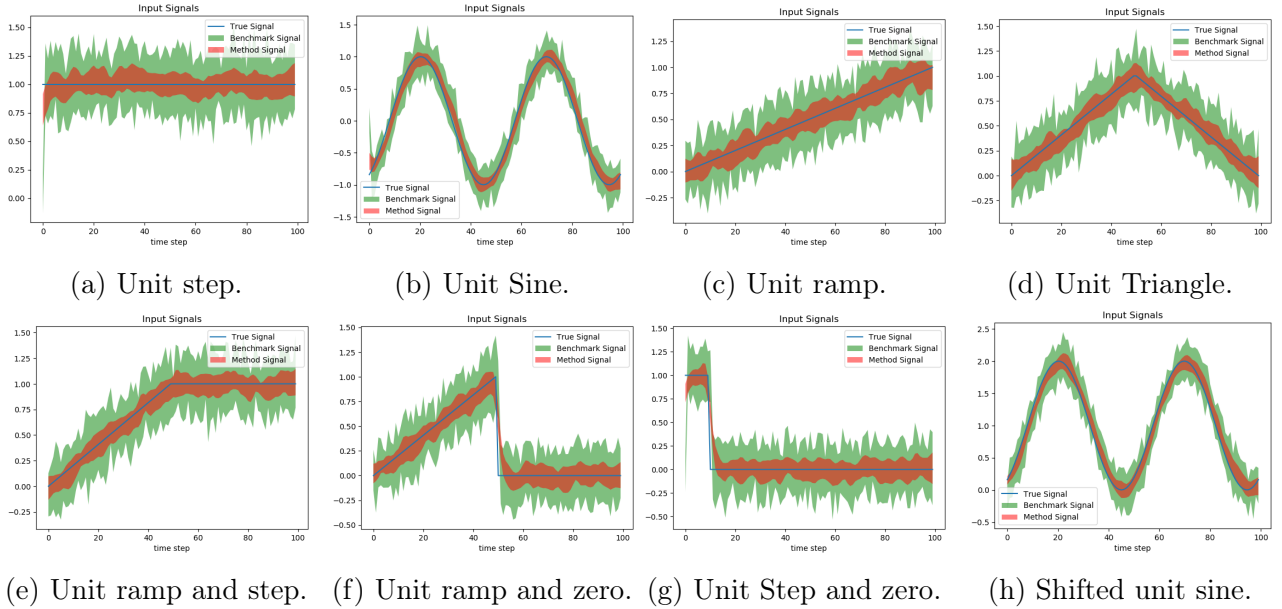


Figure 6: Input signal estimations on email server system.

Table 5: RMS error in input estimation on email server system.

	(a)	(b)	(c)	(d)
AdaL-IE	<b><math>0.112 \pm 0.016</math></b>	<b><math>0.139 \pm 0.016</math></b>	<b><math>0.123 \pm 0.015</math></b>	<b><math>0.113 \pm 0.012</math></b>
UMV-IE	$0.325 \pm 0.018$	$0.334 \pm 0.017$	$0.317 \pm 0.030$	$0.310 \pm 0.023$
	(e)	(f)	(g)	(h)
AdaL-IE	<b><math>0.111 \pm 0.007</math></b>	<b><math>0.131 \pm 0.014</math></b>	<b><math>0.137 \pm 0.012</math></b>	<b><math>0.140 \pm 0.018</math></b>
UMV-IE	$0.312 \pm 0.023$	$0.320 \pm 0.017$	$0.345 \pm 0.027$	$0.324 \pm 0.019$

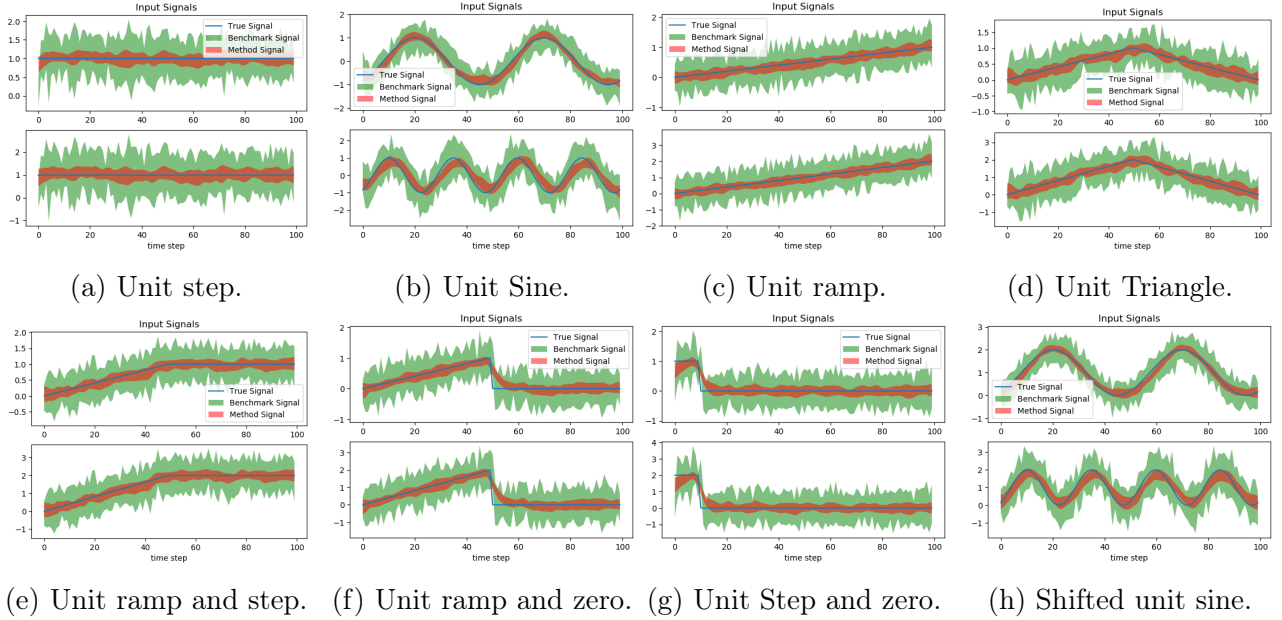


Figure 7: Input signal estimations on HTTP server system.

Table 6: RMS error in input estimation on HTTP server system.

	(a)	(b)	(c)	(d)
AdaL-IE	<b><math>0.234 \pm 0.041</math></b>	<b><math>0.318 \pm 0.038</math></b>	<b><math>0.241 \pm 0.021</math></b>	<b><math>0.255 \pm 0.028</math></b>
UMV-IE	$0.885 \pm 0.057$	$0.887 \pm 0.063$	$0.898 \pm 0.064$	$0.869 \pm 0.062$
	(e)	(f)	(g)	(h)
AdaL-IE	<b><math>0.239 \pm 0.034</math></b>	<b><math>0.267 \pm 0.032</math></b>	<b><math>0.274 \pm 0.038</math></b>	<b><math>0.305 \pm 0.044</math></b>
UMV-IE	$0.859 \pm 0.070$	$0.889 \pm 0.048$	$0.910 \pm 0.068$	$0.897 \pm 0.064$

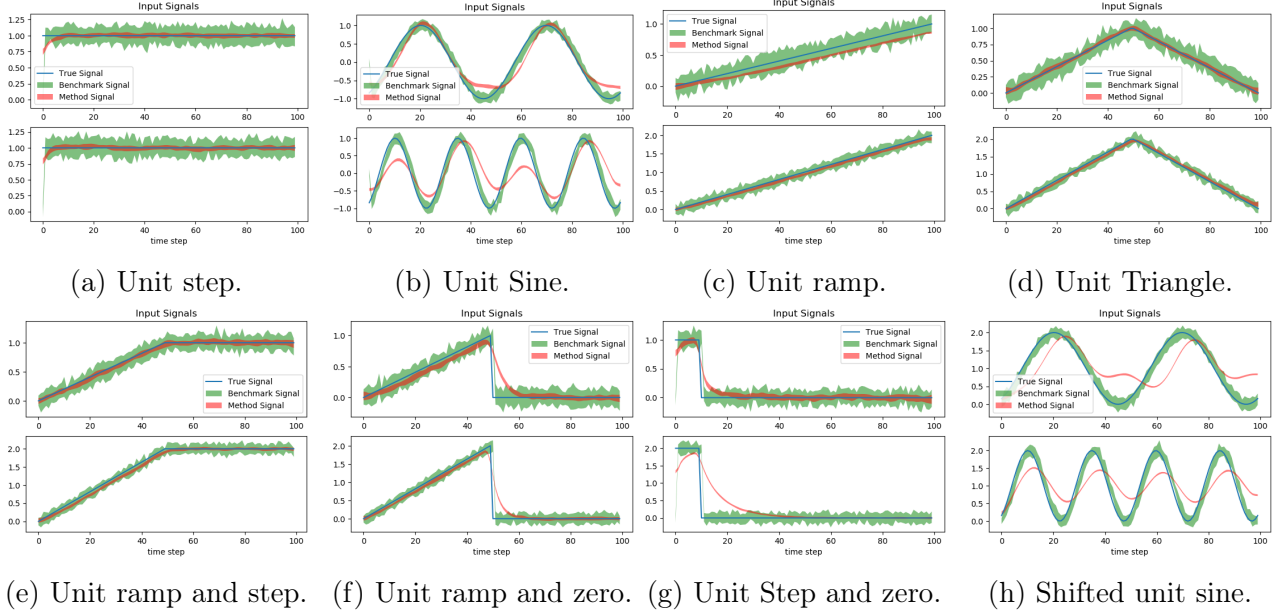


Figure 8: Input signal estimations on random system.

Table 7: RMS error in input estimation on random system.

	(a)	(b)	(c)	(d)
AdaL-IE	<b><math>0.049 \pm 0.005</math></b>	$0.375 \pm 0.006$	<b><math>0.085 \pm 0.006</math></b>	<b><math>0.056 \pm 0.006</math></b>
UMV-IE	$0.188 \pm 0.009$	<b><math>0.228 \pm 0.009</math></b>	$0.166 \pm 0.011$	$0.161 \pm 0.010$
	(e)	(f)	(g)	(h)
AdaL-IE	<b><math>0.062 \pm 0.005</math></b>	<b><math>0.163 \pm 0.006</math></b>	$0.259 \pm 0.006$	$0.533 \pm 0.003$
UMV-IE	$0.156 \pm 0.006$	$0.221 \pm 0.009$	$0.277 \pm 0.008$	<b><math>0.222 \pm 0.009</math></b>

Table 8: RMS error in input estimation on nonlinear 427 system.

	(a)	(b)	(c)	(d)
AdaL-IE	<b><math>0.237 \pm 0.067</math></b>	<b><math>0.500 \pm 0.063</math></b>	<b><math>0.257 \pm 0.042</math></b>	<b><math>0.285 \pm 0.049</math></b>
UMV-IE	$1.673 \pm 0.124$	$1.678 \pm 0.123$	$1.674 \pm 0.103$	$1.677 \pm 0.133$
	(e)	(f)	(g)	(h)
AdaL-IE	<b><math>0.261 \pm 0.054</math></b>	<b><math>0.297 \pm 0.058</math></b>	<b><math>0.290 \pm 0.049</math></b>	<b><math>0.533 \pm 0.073</math></b>
UMV-IE	$1.681 \pm 0.125$	$1.653 \pm 0.151$	$1.651 \pm 0.094$	$1.676 \pm 0.109$



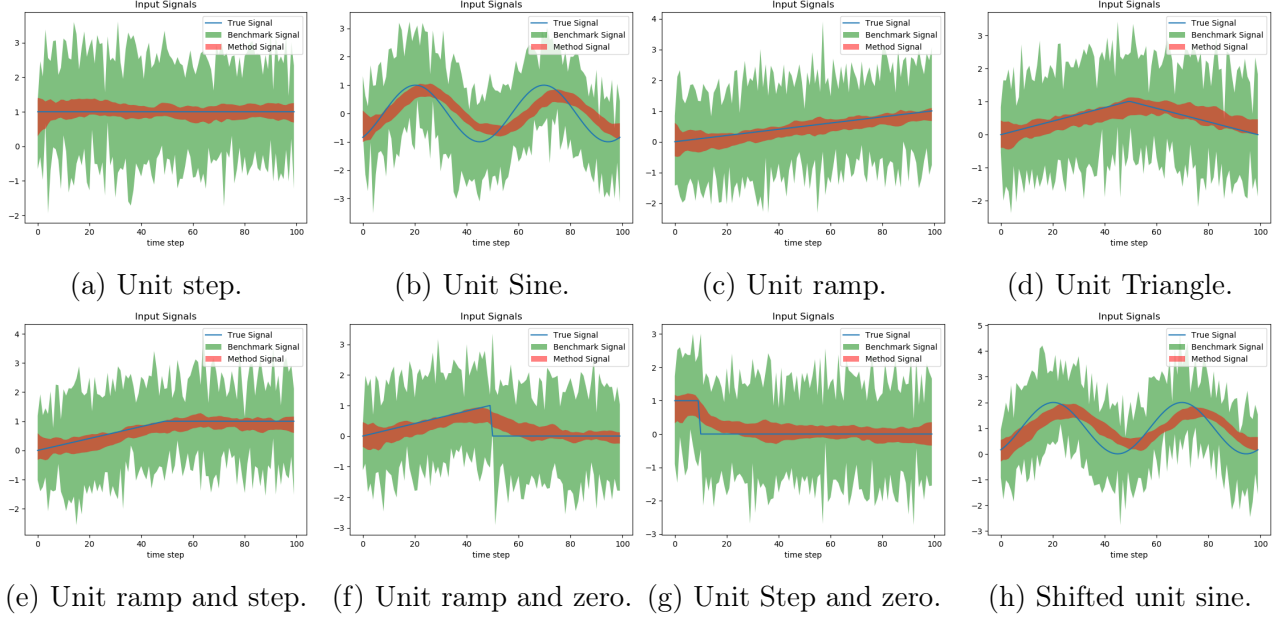


Figure 9: Input signal estimations on nonlinear 427 system.

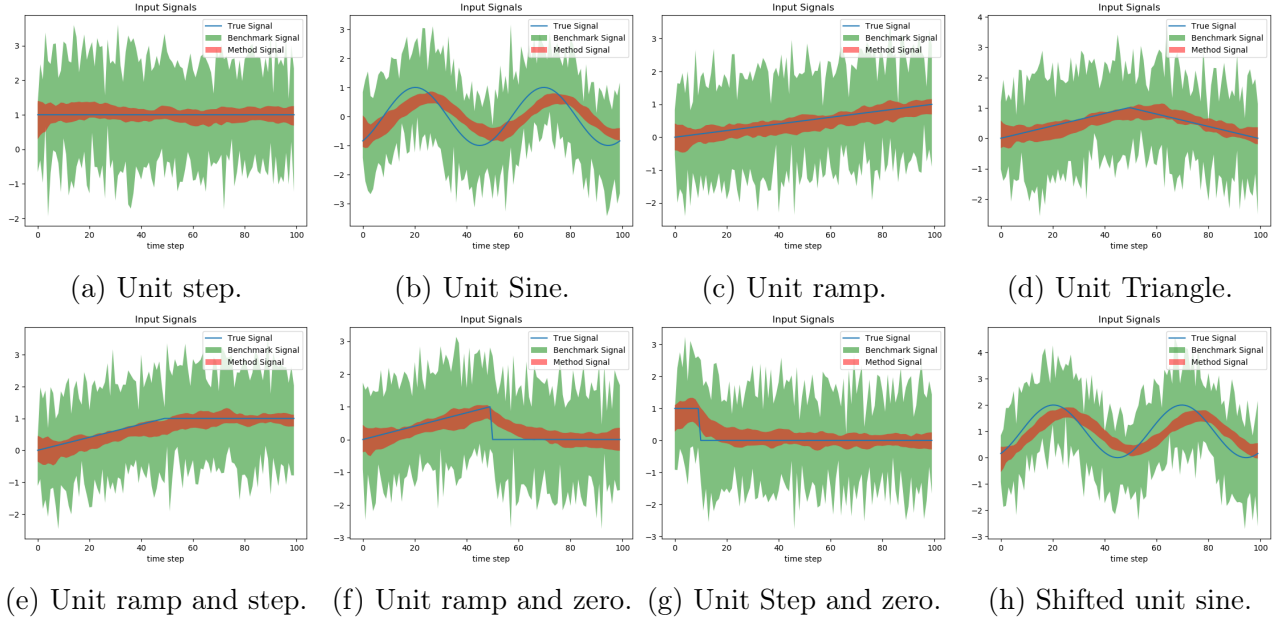


Figure 10: Input signal estimations on nonlinear 461 system.

Table 9: RMS error in input estimation on nonlinear 461 system.

	(a)	(b)	(c)	(d)
AdaL-IE	<b><math>0.237 \pm 0.066</math></b>	<b><math>0.500 \pm 0.067</math></b>	<b><math>0.263 \pm 0.036</math></b>	<b><math>0.259 \pm 0.054</math></b>
UMV-IE	$1.673 \pm 0.124$	$1.677 \pm 0.106$	$1.677 \pm 0.132$	$1.681 \pm 0.125$
	(e)	(f)	(g)	(h)
AdaL-IE	<b><math>0.266 \pm 0.061</math></b>	<b><math>0.307 \pm 0.063</math></b>	<b><math>0.294 \pm 0.049</math></b>	<b><math>0.515 \pm 0.061</math></b>
UMV-IE	$1.645 \pm 0.153$	$1.650 \pm 0.092$	$1.676 \pm 0.115$	$1.701 \pm 0.131$